

INTEGRATION OF ENHANCED HORIZONTAL DERIVATIVE FILTERING AND SHADED RELIEF DISPLAY AS AID TO LINEAMENT MAPPING ON POTENTIAL FIELD IMAGES

G.C. ONYEDIM⁺ and M.O. AWOYEMI

Department of Physics, Obafemi Awolowo University, Ile-Ife, Nigeria.

(Submitted: 26 August 2005; Accepted: 17 November 2005)

Abstract

Potential field maps are traditionally displayed in the form of contours. The identification of lineaments on such maps can be subjective and tedious particularly if the sources of the linear features do not possess appreciable differences in density or magnetic susceptibility. In such a case, the enhanced horizontal derivative (EHD) function can be used to identify the exact locations of lineaments. However, if the dynamic range of the field intensities is dominated by low values, contour displays of the derivative field become bland and only the very prominent linear features can be detected. The shaded relief display (SRD) or its colour equivalent, the colour shaded relief display (CSRD) technique, which simulates the shadowing effects of the sun on topography, can provide the dynamic range required to enhance even the very subtle lineaments.

This paper describes the utility of integrating the enhanced horizontal derivative function and the shaded relief display technique for mapping linear features on potential field maps. The synthetic magnetic field of a buried prism and the aeromagnetic map of part of Ilesha area, southwestern Nigeria, were analysed to demonstrate the effectiveness of the method.

Keywords: Potential fields, enhanced horizontal derivative, shaded relief display, lineaments.

1. Introduction

Naturally occurring lineaments observed on geophysical and topographic maps and remote sensing images are known to represent joints, faults, folds, shear zones, linear intrusives, lithologic boundaries and linear topographic features. Detection and mapping of lineaments is an important operation in exploration and environmental studies: for the study of the structural or tectonic history of a region, to aid detection of seismic horizons, investigation of active fault patterns, exploration for petroleum and solid mineral deposits and groundwater resources, etc.

Potential field data are usually displayed in the form of contour maps on which lineaments can be identified as any kind of linear or sublinear feature or alignment of features in the contour pattern (Frost, 1977; Onyedim and Ogunkoya, 2002). These include: straight line contour patterns with a steep gradient relative to the surrounding gradients; alignment of maxima and/or minima; alignment of flattened terminations of maxima and/or minima and any combination of the three.

Therefore in order to map lineaments from potential field data, it is first necessary to estimate the locations of the contacts. This is done by constructing from the data a function that is peaked over the contacts.

Several such functions have been suggested in the literature including: the horizontal gradient magnitude (HGM) (Cordell and Grauch, 1985; Blakely and Simpson, 1986); the analytic signal (AS) amplitude (Nabighian, 1984; Roest *et al.*, 1992), the local wave number (LWN) (Smith *et al.*, 1998) and the enhanced horizontal derivative (EHD) (Fedi and Florio, 2001).

Contour displays of the derivative functions may not portray the lineaments sufficiently for quick identification because only the largest values corresponding to the highest amplitude source edges will be visible on the contours. Consequently, maps of the HGM, AS, LWN and EHD require a better display technique for exhibiting the full dynamic range of the data. The shaded relief display (SRD) or the colour shaded relief display (CSRD) (Broome, 1990) can provide that dynamic range.

This paper uses a synthetic and a field example to illustrate how a combination of the EHD filter and SRD can enhance and facilitate the identification of lineaments on magnetic maps. Applications to the magnetic field of a buried prism and the aeromagnetic map of part of Ilesha area, southwestern Nigeria are presented to illustrate the effectiveness of the method.

⁺ corresponding author (email: gonyedim@oauife.edu.ng)

2. Theory

(a) The enhanced horizontal derivative (EHD) filter
The HGM, AS and LWN methods appear to lack resolution in a multi-source situation due to the interference effects from nearby sources. The magnetic map of an area is an integration of the contributions from the magnetic effects of several sources. Therefore, Fedi and Florio (2001) suggested the use of the enhanced horizontal derivative (EHD) as a better and high-resolution boundary analysis technique.

According to Fedi and Florio (2001), if $f(x,y,z_0)$ represents the observed field or its derivative on a defined surface located at height $z=z_0$, then we can define a new function $\Phi(x,y,z_0)$ as the sum:

$$\Phi(x,y,z_0) = f(x,y,z_0) + f^1(x,y,z_0) + f^2(x,y,z_0) + \dots + f^m(x,y,z_0) \tag{1}$$

where $f^n(x,y,z_0)$ is the n^{th} vertical derivative of $f(x,y,z_0)$. Then the EHD is given as the magnitude of the horizontal derivative of $\Phi(x,y,z_0)$, thus:

$$EHD(x,y,z_0) = \left[\left(\frac{\partial \Phi}{\partial x} \right)^2 + \left(\frac{\partial \Phi}{\partial y} \right)^2 \right]^{1/2} \tag{2}$$

The maxima of horizontal derivatives of the higher-order terms in Eqn.1 are located over the source corners while those of the lower-order derivatives define the main lineaments of the sources. Therefore we limited the terms in $\Phi(x,y,z_0)$ to the second order vertical derivative.

The computation of high order derivatives, as required in Eqn.1 must be given some attention because the process is inherently prone to noise amplification, particularly if the vertical derivative is calculated using a frequency-domain filter operator (Gunn, 1975). Noting that the second vertical derivative of the magnetic field is related to the two second horizontal derivatives according to Laplace's equation,

$$\frac{\partial^2 f}{\partial z^2} = - \left(\frac{\partial^2 f}{\partial x^2} + \frac{\partial^2 f}{\partial y^2} \right) \tag{3}$$

we computed the former through the finite difference representations of the latter. This method is more stable than the frequency domain Fourier horizontal derivative operators.

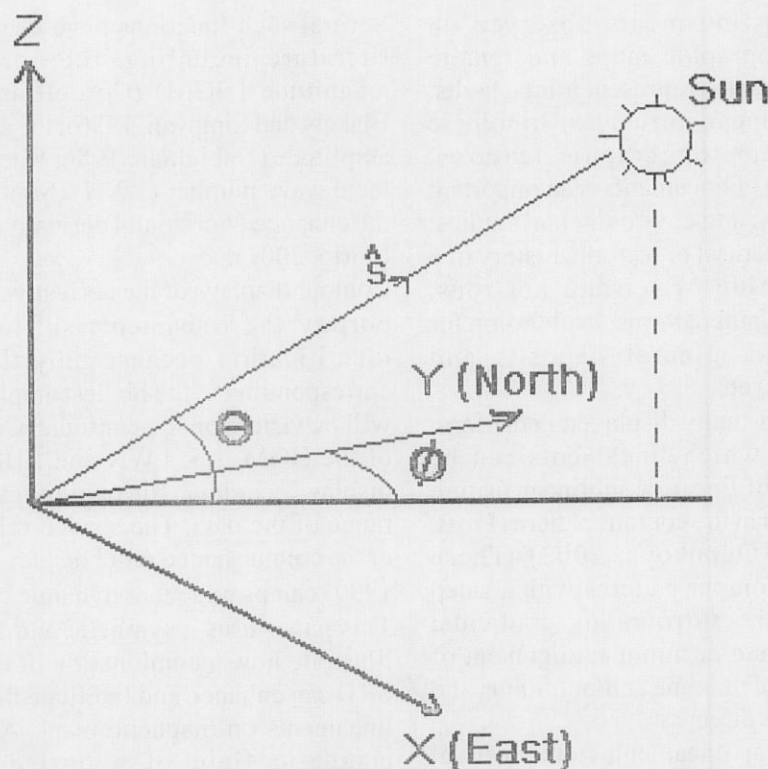


Fig.1 Schematic diagram showing parameters used to compute the shaded relief effect for an illumination source with elevation θ and azimuth ϕ .

(b) Shaded relief technique

The shaded relief technique, also referred to as sun shading (Cooper, 2003), has been used for many years for displaying geophysical data, including gravity and magnetic data (Paterson and Reeves, 1985; Kowalik and Glenn, 1987), synthetic aperture radar data (Sabins, 1998), and the interpreted 3-D seismic horizons (Hoetz and Watters, 1992). Because of the imaging style of the Side Looking Airborne Radar (SLAR) and the Synthetic Aperture Radar (SAR) systems, the resulting images have a shadowing effect which is similar to that on the shaded relief map.

Shaded relief images are produced by simulating a photographic imaging of a digitally-stored grid, thus transforming geophysical data into apparent illuminated topography. The technique treats the potential field data as if it were a topographic surface, and uses an artificial light source to create the impression of shadows that 'accentuate' the 'topography' of the potential field map.

The method used to produce a shaded relief image depends on the physical model adopted out of a variety of algorithms available (Horn, 1982). For our purpose, we employ the model of an ideal Lambertian reflector such that the surface reflects equally in all directions. The mathematical basis for this can be explained using the diagram in Fig. 1. If s is the unit vector pointing towards the light source, with declination ϕ (clockwise from North) and elevation θ (measured from the horizon) and if I is the unit vector normal to the particular element of surface defined by the potential function ψ of interest, such as the total intensity field, the EHD, etc, then

$$s = \frac{-\frac{\partial \psi}{\partial x} i - \frac{\partial \psi}{\partial y} j + k}{\left[\left(\frac{\partial \psi}{\partial x} \right)^2 + \left(\frac{\partial \psi}{\partial y} \right)^2 + 1 \right]^{1/2}} \quad (4)$$

where i, j, k are unit vectors in the $x, y,$ and z directions respectively.

Accordingly, each surface element (pixel) on the map is then assigned a grayscale value g by

$$g = I \cdot s \quad (5)$$

where $g = 1$ corresponds to black and $g = -1$ corresponds to white. This way, the potential field function defined on the map is represented as a greyscale image. When applied to a coloured map, the result is a colour shaded relief (CSR) image.

Unlike natural relief images, the light source can be artificially manipulated to shine from a user-defined direction so that even the very subtle linear features can be enhanced on the basis of strike direction.

Thus, shaded relief enhances lineaments perpendicular to the illumination direction and suppresses features parallel to it. Different illumination directions reveal lineaments with different strike directions so that shaded relief acts as a simple but effective directional filter.

3. Application to synthetic and field data

(a) Synthetic example

We first demonstrate the feasibility of the method using synthetic anomaly data of a 35km x 35km bottomless prism whose upper surface is 3km deep. The magnetic anomaly values were calculated at the intersection of grid lines spaced 0.5km apart over a 55km x 55km area whose centre coincides with that of the prism. The ambient magnetic field of intensity 32,000 nT and the remanent magnetization vector have inclination and declination of 40° and 20° respectively. Shaded relief images of the magnetic field and the RTP and EHD conversions are shown in Figs. 2a and b respectively. Since the sides of the prism trend north-south and east-west, only two illumination directions, 0° and 90° at an elevation of 30° were used for the SRD as shown in Fig. 2c and d respectively. The images of the EHD field demonstrate how precisely the maxima are located directly over the edges of the prism. Thus, linear basement faults or lateral terminations of magnetic bodies produce correspondingly linear observed magnetic gradients that can be imaged in the same manner.

(b) Field example

The field example is a 28 km x 28 km area located southeast of Ilesha and bounded by longitudes 4° 45' and 5° 00' and latitudes 7° 30' and 7° 45'. The area was chosen for two reasons: firstly, a lineament map produced by interpreting SPOT imagery is available for comparison; secondly, the rocks in the area are mainly migmatites, gneisses, quartzites and granites, which, except for some granites, have low magnetic susceptibility. In this case, it is necessary to employ enhancement techniques to amplify the very subtle anomalies due to lineaments associated with contacts and faults.

The data used in the study was taken from sheet 243 S 1 of the *Geological Survey of Nigeria*. The map was digitized by interpolating the contour values onto a square grid at 1 km spacing. A contour map of the total intensity magnetic field is shown in Fig. 3a.

(c) Processing of aeromagnetic data

On a gravity map, positive anomalies occur directly above mass concentrations, but for magnetic anomalies, this is not the case as both the geomagnetic field and magnetization direction of the anomalous body are in general not vertical. Consequently, magnetic anomalies are typically

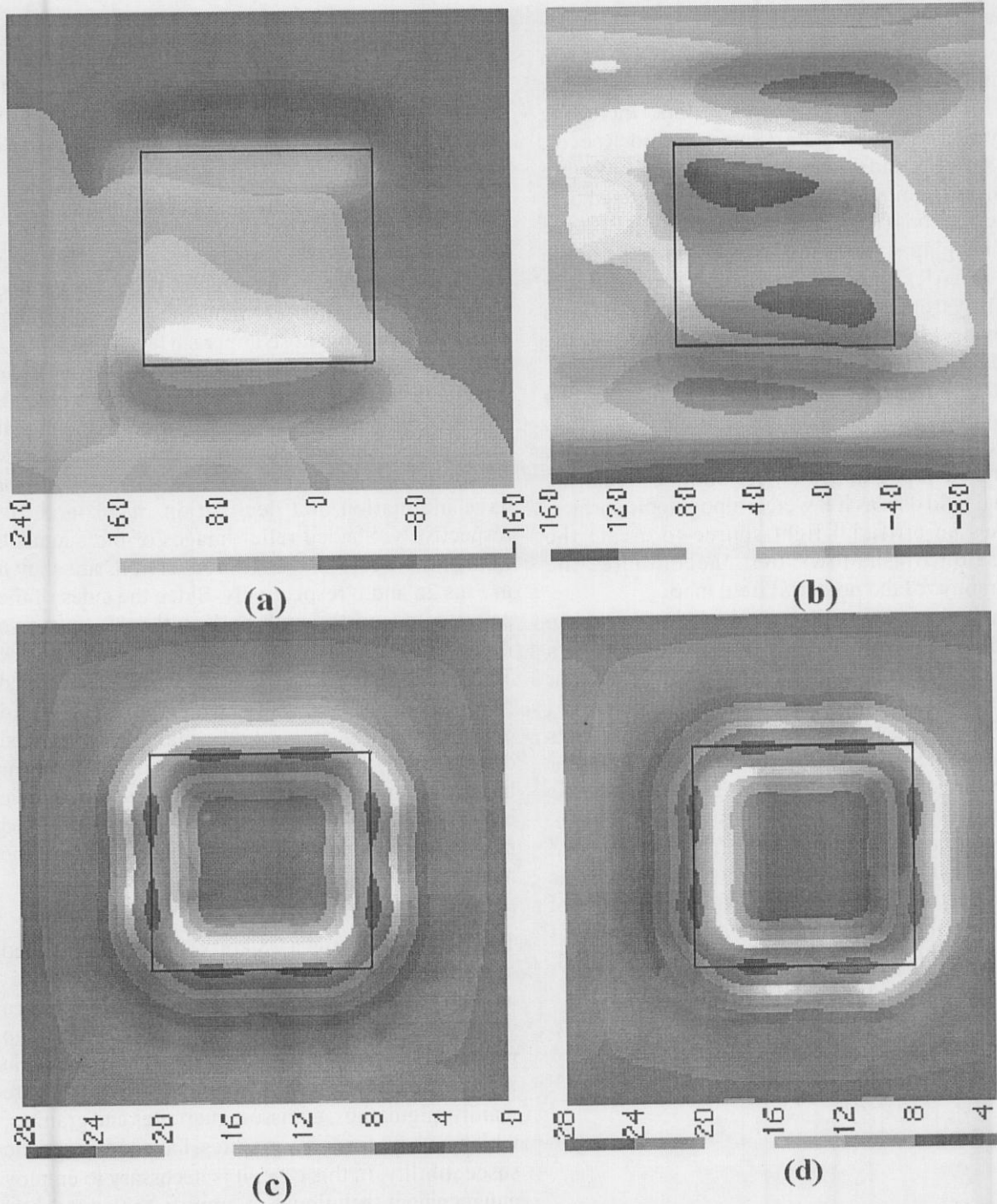


Fig.2. Synthetic magnetic anomaly over a vertical prism (a) total intensity (nT), (b) RTP (nT) field and (c) the EHD of the RTP field (nT/km).

shifted laterally from the causative body and contain both positive and negative components. One way to simplify the dipolar shapes of magnetic anomalies is to apply a reduction-to-the-pole (RTP) filter. This way, the magnetic field is reduced to that which would be observed if the survey area were located at the pole where the induced magnetization and the ambient field are both directed vertically downwards (Blakely, 1995).

In relatively low magnetic latitudes such as Ilesha area, the RTP operator can become unstable because

the amplitude correction factor for north-south trending features unreasonably amplifies noise and severely distorts magnetic anomalies from sources magnetized in directions different from that of the inducing field. In this study, RTP was carried out in the frequency domain and, to minimize the distortions described above, the Fourier coefficients were modified using a tapered azimuthal filter as described by Hansen and Pawlowski (1989) and Mendonca and Silva (1993). The RTP magnetic field of the study area is shown in Fig.3b.

(d) Identification of lineaments

Side lighting (non-vertical illumination) acts as a directional filter, enhancing anomalies non-parallel to the 'sun' azimuth. Therefore, many shaded relief maps with different illumination source azimuths are required to reveal lineaments with different strike directions that exist in an area. In this study, shaded relief maps were generated for illumination source from the north, northeast, east and southeast so as to highlight linear features trending E-W, NW-SE, N-S and NE-SW respectively. Illumination from the south, southwest, west and northwest will produce the same effects respectively. In all the cases, a sun elevation angle of 30° was applied. However, in order to show the advantage of side lighting, an image for a sun elevation of 90° was included for comparison. An interpreter of a shaded relief image needs to keep the sun's position in mind while picking linear trends. For example, if the sun is in the northeast, the lineament locations are picked where a bright slope

facing the northeast turns to a dark southwest slope. The theoretical line of the lineament is the ridge where the light turns to dark. Based on this criterion, a lineament map for the area was produced by placing a transparent sheet over a hard copy of each image in turn and marking out the boundary between the bright and dark slopes.

4. Discussion

Any attempt to interpret lineaments from the dipolar and the RTP contour maps in Fig.3 using the criteria outlined earlier would produce few and subjective results. Furthermore, the EHD process has produced elongated closed contour patterns in places but there identification still requires a lot of effort. Therefore, if we compare the contour displays in Fig.3 with the SRD in Fig.4 the advantage of the latter for identification of lineaments is immediately obvious. Fig.4a shows the case when illumination is from the north. As expected, features which strike E-W or

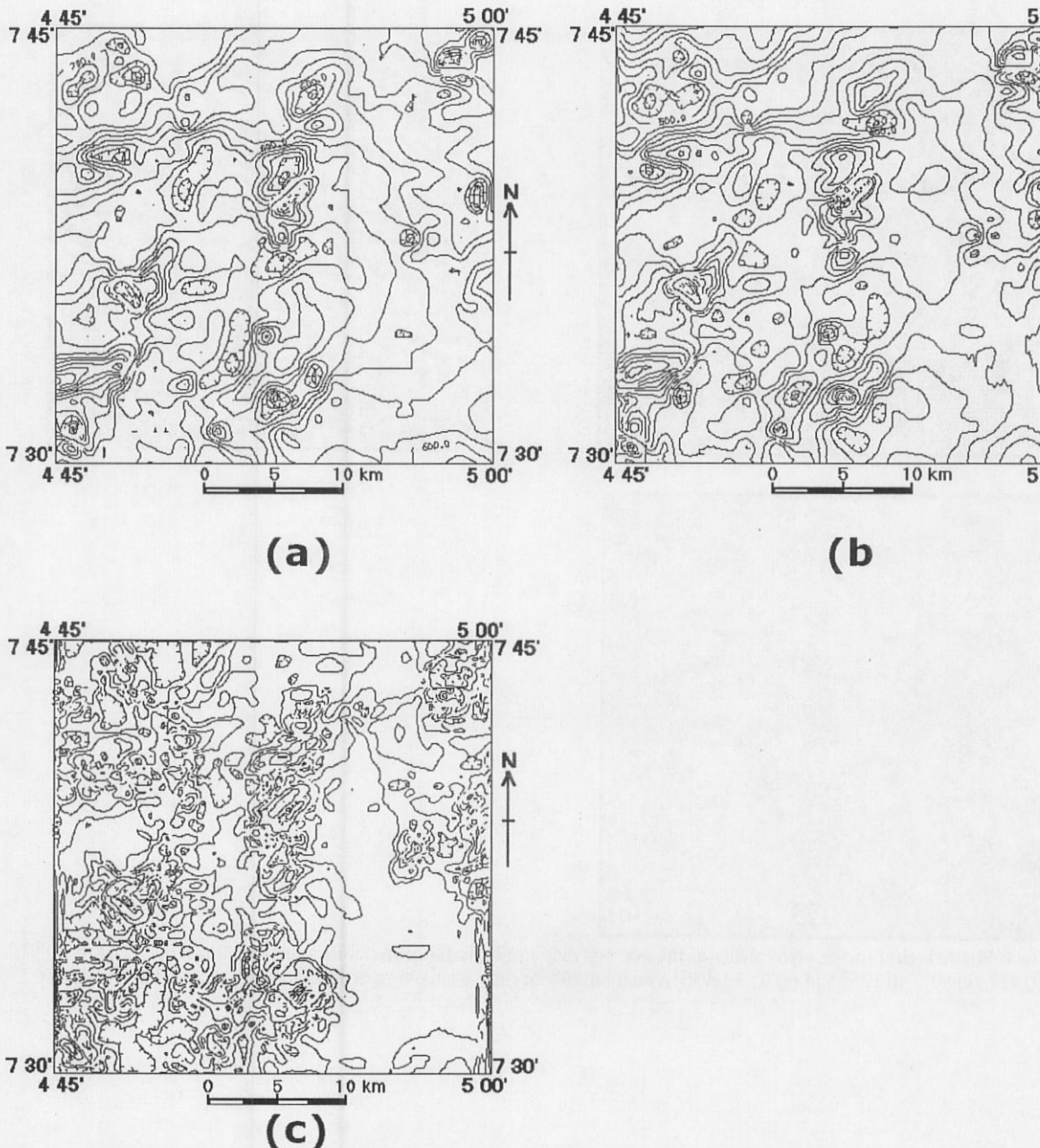


Fig.3: Contour maps of the (a) total intensity, (b) RTP and (c) EHD of RTP magnetic field of part of Ilesha area.

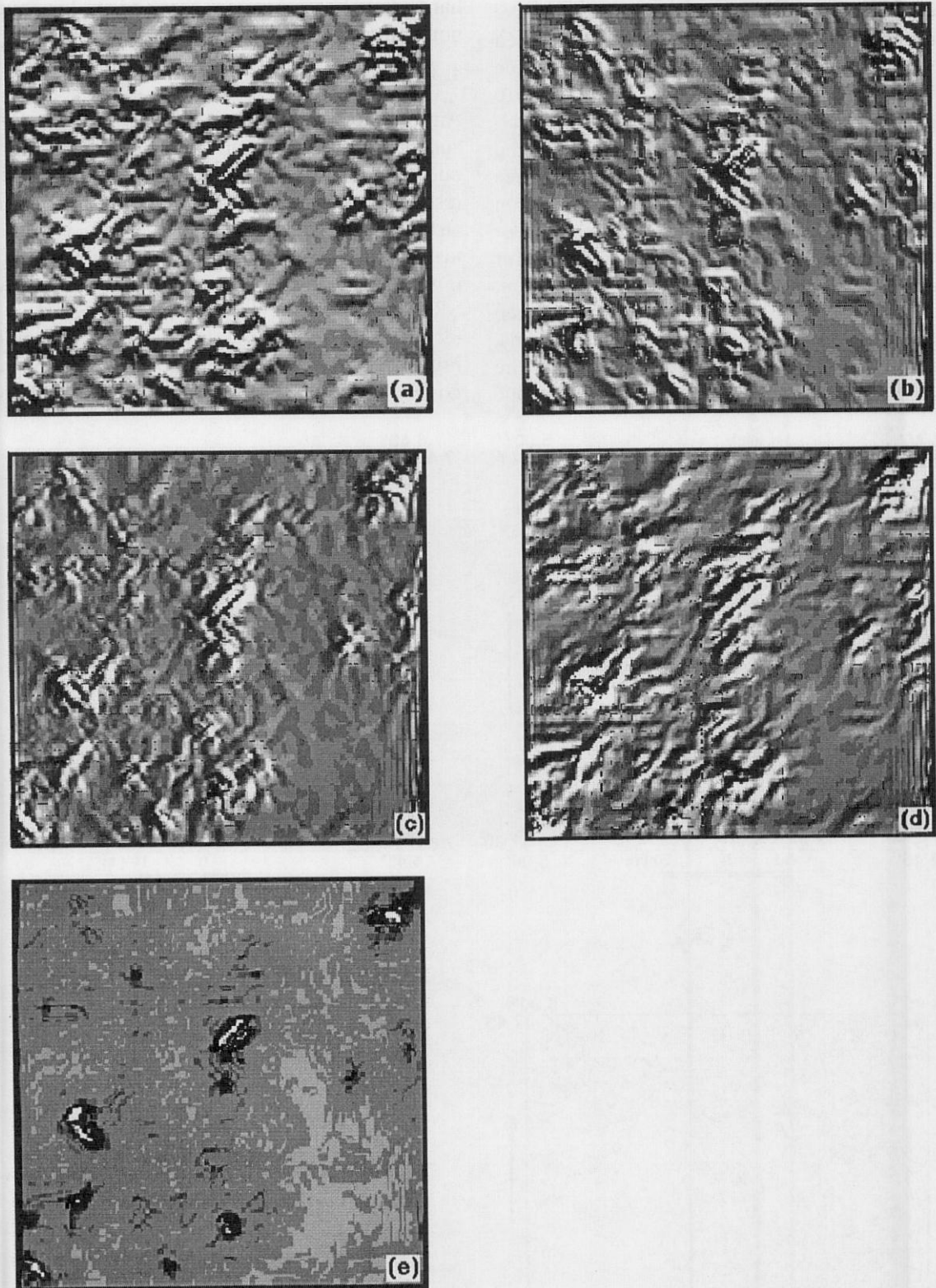


Fig.4: Shaded relief image equivalents of the contour map in Fig.3c for artificial illumination azimuths equal to (a) 0° , (b) 45° , (c) 90° , (d) 135° and (e) 0° . Elevation angle is 30° for (a)-(d) and 90° (vertical) for (e).

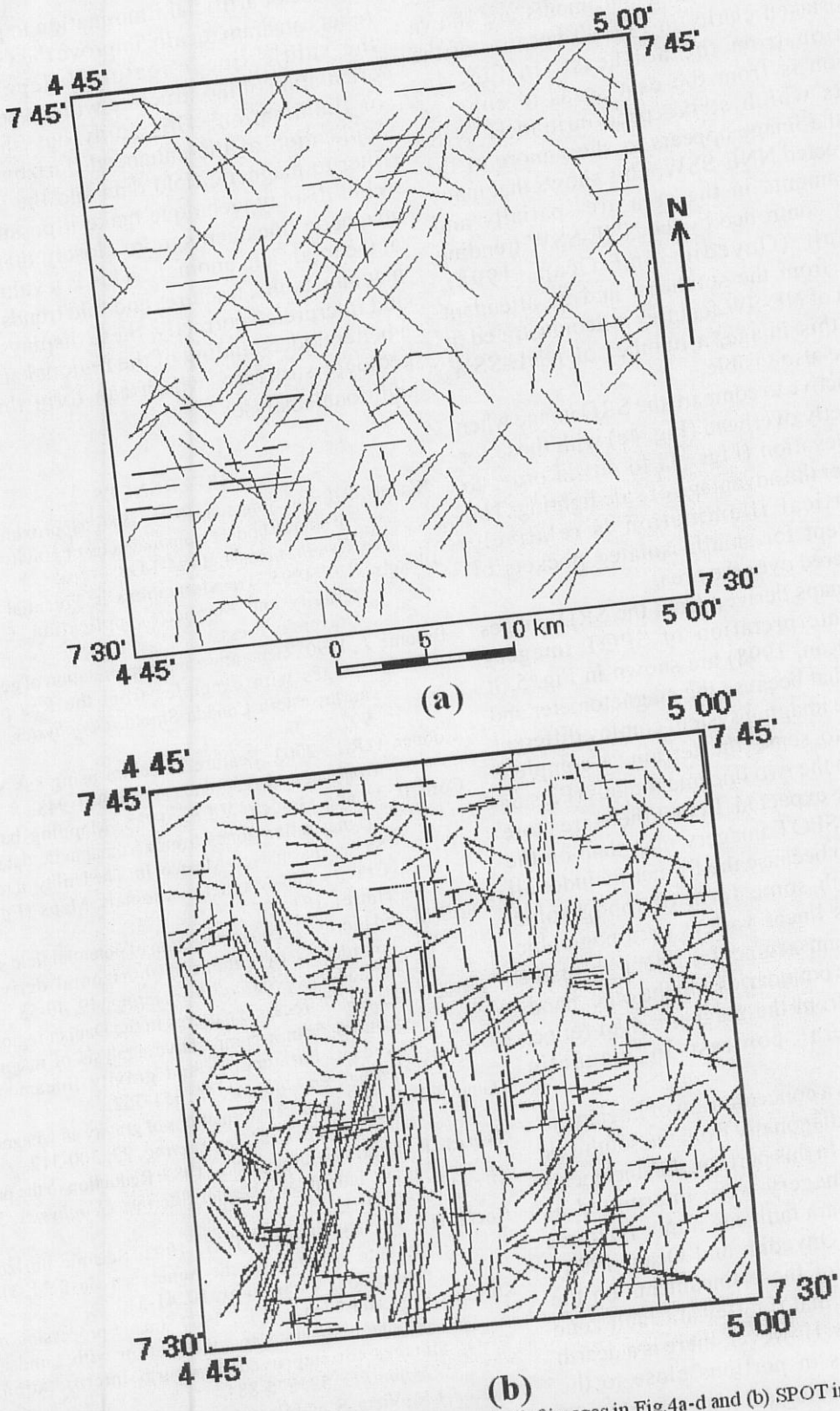


Fig.5: Lineaments interpreted from (a) shaded relief images in Fig.4a-d and (b) SPOT image of the same area (after Onyedim and Ocan, 1998).

nearly so are emphasized and can be identified easily by marking out the boundaries between the illuminated and dark regions on the SRD image. Similarly, NW-SE trending lineaments are shown with unmistakable clarity in Fig. 4b because of the illumination from the northeast. In Fig. 4c, lineaments which strike predominantly N-S. However, the image appears to show more of the features directed NNE-SSW. This shows that many of the lineaments in the area are spatially and directionally controlled by the NNE-SSW trending Ifewara fault (Onyedim and Ocan, 1998). Illumination from the southeast and its attendant enhancement of NE-SW features is demonstrated in Fig. 4d. On this image, a number of NNE-SSW lineaments are also visible.

It is also instructive to compare the SRD image when the sun is directly overhead (Fig. 4e) with those for non-vertical elevation (Figs. 4a to 4d) in order to appreciate better the advantage of side lighting. The image for vertical illumination is relatively featureless except for small, isolated pockets of anomalies scattered over the area.

The lineament maps derived from the SRD images and from the interpretation of SPOT imagery (Onyedim and Ocan, 1998) are shown in Fig. 5. It should be noted that because the magnetometer and the SPOT satellite imaging system employ different types of signals to sense the terrain, a complete similarity between the two lineament maps (Figs. 5a and 5b) is not to be expected. In fact there are more lineaments on the SPOT imagery map than on the EHD magnetic map because the former includes all linear features with some form of topographic expression, such as linear valleys or topographic highs, straight stream segments, linear intrusive bodies and lithologic boundaries. On the other hand, lineaments derived from the magnetic map reflect features with lateral contrast in magnetic susceptibility.

On both maps, there is a concentration of lineaments within a belt that runs diagonally from the southwest to the northeast corner. In this portion, the lineaments observed on SPOT imagery were interpreted as expressions of the Ifewara fault and minor fractures within the fault zone (Onyedim and Ocan, 1998). The strong expression of these lineaments on the magnetic map suggests that the Ifewara fault zone has a magnetic signature. However, there is a dearth of magnetic lineaments in portions close to the eastern boundary. The geological map for this area shows that these portions are underlain by quartzite ridges, which have relatively very low magnetic susceptibility. On the SPOT imagery lineament map (Fig. 5b), the ridges appear prominently where they are expressed as N-S to NNE-SSW trending

topographic lineaments.

5. Conclusion

The use of artificial illumination to produce shaded relief can dramatically improve the visibility of even the subtle linear features, depending on the orientation of the structure with respect to the angle of illumination. This study has shown that the application of the enhanced horizontal derivative filter to magnetic field data and the use of shaded relief display technique make it possible to follow magnetic lineaments more closely than by looking at the total field anomaly. This is a valuable tool for mapping faults, fractures and fold trends. When used and interpreted correctly, these displays can lead to a better understanding of the regional and localized geologic structure, which can form the basis for additional analyses.

REFERENCES

- Blakely, R.J. and Simpson, R.W., 1986. Approximating edges of source bodies from magnetic or gravity anomalies. *Geophysics*, 51, 1494-1498.
- Blakely, R.J., 1995. Transformations in Potential Theory in Gravity and Magnetic Application. Cambridge University Press.
- Broome, J., 1990. Generation and interpretation of geophysical images with examples from the Rea province, northwestern Canada Shield. *Geophysics*, 55, 977-997.
- Cooper, G.R.J., 2003. Feature detection using sun shading. *Computers & Geosciences*, 29, 941-948.
- Cordell, L. and Grauch, V.J.S., 1985. Mapping basement magnetization zones from aeromagnetic data in the Sa Juan basin, New Mexico. In: *The Utility of regional Gravity and Magnetic Anomaly Maps* (Ed. W.J. Hinze), 181-197.
- Fedi, M. and Florio, G., 2001. Detection of potential field source boundaries by enhanced horizontal derivative method. *Geophysical Prospecting*, 49, 40-58.
- Frost, R.T.C., 1977. Tectonic patterns in the Danish region (as deduced from a comparative analysis of magnetic, Landsat, bathymetric and gravity lineaments). *Geologie en Mijbouw*, 56, 351-362.
- Gunn, P.J., 1975. Linear transformations of gravity and magnetic fields. *Geophysical Prospecting*, 23, 300-312.
- Hansen, R.O. and Pawlowski, R.S., 1989. Reduction to the pole at low latitudes by Weiner filtering. *Geophysics*, 54, 1607-1613.
- Hoetz, H.L.J.G. and Watters, D.G., 1992. Seismic horizon attribute mapping for the Annerveen Gasfield, The Netherlands. *First Break*, 10, 41-51.
- Kowalik, W.S. and Glenn, W.E., 1987. Image processing of aeromagnetic data and integration with Landsat images for improved structural interpretation. *Geophysics*, 52, 875-884.
- Macleod, I.N., Viera, S. and Chaves, A.C., 1993. Analytic signal and reduction-to-the-pole in the interpretation of total magnetic field data at low latitudes. Proc. of the Third International Congress of the Brazilian Society of Geophysicists, 830-855.
- Mendonca, C.A. and Silva, B.C., 1993. A stable truncated series approximation of the reduction-to-the-pole operator. *Geophysics*, 58, 1084-1090.
- Nabighian, M.N., 1984. Towards the three-dimensional automatic interpretation of potential field data via

- generalized Hilbert transforms: Fundamental relations. *Geophysics*, 53, 957-966.
- Onyedim, G.C. and Ocan, O.O., 1998. Characteristics and tectonic significance of SPOT imagery lineaments around part of Ifewara fault, southwestern Nigeria. *Africa Geoscience Review*, 5, 499-506.
- Onyedim, G.C. and Ogunkoya, O.O., 2002. Identification and geological significance of lineaments and curvilinear features on topographic maps. *Journ. Min. Geol.*, 38, (1), 13-20.
- Paterson, N.R. and Reeves, C.V., 1985. Application of gravity and magnetic surveys: the state-of-the-art in 1985. *Geophysics*, 50, 2558-2594.
- Roest, W.R., Verhoef, J. and Pilkington, M., 1992. Magnetic interpretation using 3-D analytic signal. *Geophysics*, 57, 116-125.
- Sabins, F.F., 1998. *Manual of Remote Sensing: Principles and Applications of Imaging Radar*. New York; Chichester: J. Wiley.
- Smith, R.S., Thurston, J.B., Dai, Ting-Fan and MacLeod, I.N., 1998. iSPI™-the improved source parameter imaging method. *Geophysical Prospecting*, 46, 141-151.